Journal of Inorganic and Organometallic Polymers and Materials (2024) 34:1282–1292
https://doi.org/10.1007/s10904-023-02889-1

RESEARCH

Catalytic and Antioxidant Activity of *Desmarestia menziesii* Algae Extract Based Organic@İnorganic Hybrid Nanoflowers

Fatih Doğan Koca[1] · Haydar Matz Muhy[2] · Mehmet Gökhan Halici[3]

Received: 2 June 2023 / Accepted: 22 September 2023 / Published online: 23 October 2023

Abstract

There are numerous studies about on nanoparticle synthesis by reducing metal salts via bio-extracts. Organic@inorganic hybrid nanoflowers (hNFs), are synthesized with expensive molecules such as enzymes, DNA and proteins. There are few studies for synthesis of hybrid nanoflowers via bio-extracts. However, the use of algae extracts as an organic component and studies on potential applications are very few. For the first time, the algae extract obtained from the brown macroalgae *Desmarestia menziesii* was used as the organic component of hNFs. Effect of medium pH, and algal extract concentration on morphological characteristic of hNFs were evaluated. The dye degradation and antioxidant activities of hNFs synthesized under optimum conditions were determined. hNFs were not synthesized in the acidic conditions of the PBS buffer (pH 5), The synthesis of hNFs was realized with coordination of Cu^{+2} and algae extract (0.65, 1, and 1.65 mL) in PBS (pH 7.4 and 9). hNFs with ideal flower morphology (size: 16–19 µm) were obtained by using 1.65 mL of extract under pH 7.4 condition. The basic skeletons (C, O, P, Cu), presence of phosphate crystals (PO_4^{-3}) and cristalinity of hNFs were determined by EDX, FT-IR and XRD, respectively. Antioxidant activity of hNFs against DPPH were determined depending on concentration (IC_{50}: 950 µg/ mL). The highest catalytic activities of hNFs against methylene blue and brilliant blue dyes were observed at the mediums of pH 7 (69.81%) and pH 5 (75.7%), respectively. Organic@inorganic hNFs were synthesized by using brown macroalgae *D. menziesii* depending on extract concentration and medium pH. According to our findings, these hNFs are suitable for using as catalyst and antioxidant agents.

Keywords Nanoflower · Copper · Algal extract · Catalyst · Antioxidant

1 Introduction

With the increase of nanotechnological studies and the inclusion of other disciplines, the synthesis methods (chemical, physical and biological) and application areas applied for the synthesis of nanomaterials develop day by day. In the last decade, as an alternative to synthesis of nanomaterials with chemical agents which is expensive and which may have toxic properties, green technology method became more attractive which is done by using the roots, bodies, leaves, flowers and fruits of various plants [1]. There are a lot of reports on green synthesis of metallic nanoparticles (NP) such as Ag, ZnO, CuO, and Ag@ZnO [1, 2]. NPs are used in various areas especially catalytic and biomedical applications. Various NPs are attractive for catalytic applications because of their characteristics such as surface charges, large surface areas, cost-effective, fast process and simple operations [3]. It is known that β-In_2S_3 quantum dots synthesized by *Camellia sinensis* extracts degraded effectively the Rhodamine B, Malachite Green, and Biebrich Scarlet dyes [4]. In addition, SnS_2 quantum dots/chitosan nanocomposites synthesized by *Azadirachta indica* extracts have strong catalytic activity against crystal violet dye [5].

Recently, the studies on determining the catalytic activities of enzyme-based hybrid nanoflowers (hNFs) are popular. The expensive and low stability of free enzymes used in many areas in the industry is disadvantageous. Various methods have been developed to overcome this problem, but unfortunately these methods are complex, expensive

✉ Fatih Doğan Koca
fatihdkoca@gmail.com

[1] Faculty of Veterinary Medicine, Erciyes University, Kayseri, Turkey

[2] Erciyes University, Institute of Science, Kayseri, Turkey

[3] Faculty of Science, Department of Biology, Erciyes University, Kayseri, Turkey

and in need of time requiring process [6]. The enzymes that become immobilized by classical enzyme immobilization methods are relatively more stable. However, with most immobilization methods, the active regions of some enzymes are partially blocked, conformational changes in enzymes and diffusion resistance between substrate and enzymes occur, and finallythe activities of the enzymes may decrease [7–10]. Ge et al., reported a new immobilization method by synthesis of enzyme-based hNFs [11]. Organic@inorganic NFs, which are popular recently, are successful in enzyme immobilization applications with the advantage of the structural properties of their surfaces, multilayered structures, reusabilities, biocompatibilities, high stabilities and high activities [8, 12–15]. Although hNFs are easily applicable, economical and efficient, hNFs may have problems such as separation, [8]. Cui et al. reported that surfactant-activated lipase-inorganic hNFs exhibited more effective activities than free lipase [7]. Researchers associated the superior activity of hNFs with the hierarchical structure and surfactants. Wen et al. recorded that the bimetal-based inorganic-caarbonic anhydrase hNFs were significantly recycled [9]. Researchers have declared that the hydrogel membrane, which was obtained by embabed hNFs in poly(vinyl alcohol)-chitosan have properties of enriched thermostability, pH stability, CO_2 capture capacity. Zhong et al. reported that lipase based hNFs could be a catalyst for biodisel production and these hNFs exhibited activity after 10 cycles [10]. Liu et al. reported that the isoorotic acid-zinc phosphate hNFs exhibited an effective antimicrobial activity against gram negative and gram -positive bacteria [16]. Researchers explained the antimicrobial activity of hNFs with generation of reactive oxygen species (ROS), synergistic effects of zinc (II), and interaction of membrane. Li et al. determined that horseradish peroxidase and glutamate oxidase based hNFs are suitable for the detection of glutamate [17]. Alhayali et al. revealed that catalase component Fe^3O^4@Cu^{2+} NFs were effective for methyl red (organic azo dye) degradation [18]. In another study, DNA-based Cu NFs were successfully applied for the detection of phenolic components [19]. Cai et al. found that DNA@NFs have high selective characteristics for bacterial detection of *Staphylococcus aureus* [20]. It is obvious that NFs can be synthesized by using DNA and enzymes.

Researchers focused on the field of green synthesis, and the morphological characteristics of nanoparticles such as size and shape in a controlled manner, and evaluation of its potential in the biomedical and environmen applications [1]. Demirbas determined the antimicrobial activity of Cu-hNFs against fish pathogen bacteria strain, which were synthesized with red orange shells and fruit extracts [21]. Ekennia et al. indicated that *Euphorbia sanguinea* extract based ZnO-NFs have degraded the malachite green dye, and the tyrosinase inhibitor effect of NFs [22]. Al Sharie et al. determined the minimum inhibition concentrations (MIC) of ZnO NF synthesized by using *Hypericum triquetrifolium* against to *Staphylococcus aureus* and *Enterococcus faecalis* at 20 µg/mL and 5 µg/mL, respectively [23]. In the same study, anticancer activity of ZnO NFs against lung cancer A549 cells was reported. In another study, researchers suggested that Cu-NFs synthesized by *Axinyssa digitata* extract can be used in antimicrobial applications [24]. Shahabadi et al. recorded the effect of wound healing (in vivo) potential of the NFs synthesized with *Echinophora platyloba* extract [25]. In the same study, antibacterial (against to *S. aureus*, *E. coli*) and antifungal activities (against to *Trichophyton rubrum, Candida albicans*, and *Aspergillus niger*) of NFs were revealed.

Although the studies on synthesis of hNFs via bioreadications are relatively limited, there are very few studies for synthesis of hNFs by using fungi, algae or lichen extracts [26–28]. *Desmarestia menziesii* extract was used for only synthesis of Ag and Au metallic NP, and there are no other studies with this algae extract based nanomaterial synthesis [29]. In the synthesis of organic–inorganic hybrid NFs, *D. menziesii* macroalgae was used for the first time as an organic component alternative to DNA and various enzymes. In this study, the algae based Cu-NFs were characterized by SEM, FT-IR and EDX analyzes and antioxidant activity against 2,2-diphenyl-1-picrylhydrazyl (DPPH) was evaluated. It was also observed that these synthesized hNFs exhibit an effective catalytic activity against methylene blue and brilliant blue. As a result, we suggest that biomaterials-based NFs can be improved and they can be applicable for biomedical and environmental application areas in the future.

2 Materials and Methods

2.1 Synthesis of Hybrid Nanoflower

Macroalgae samples (collected from Antarctica, and identified by Dr. Mehmet Gökhan Halıcı) were kept in distilled water (10 g dry/100 mL, 70 °C, 45 min) to obtain *D. menziesii* extract, which was selected as the organic input of hNFs, and then filtered via Whatman No 1 filter paper. In order to determine the effects of parameters on synthesis success and morphologies of hNFs, algae extracts were added at increasing concentrations (0.65 mL, 1 mL, and 1.65 mL) to PBS bumpers prepared at different pHs (pH 5, 7.4, and 9). After the divalent Cu (0.35 mL, 0.8 M $CuSO_4$) was added to the tubes, vortexed and incubated (3 days, in the dark). Blue precipitiors formed at the bottom of the tubes were divided via centrifulation for 10 min at 4000 rpm and was washed, and used for characterization [21]. Following the characterization of hNFs, hNFs synthesized in the closest

conditions to the ideal flower morphology according to FE-SEM were used for catalytic and antioxidant studies.

2.2 Antioxidant Activities of Hybrid Nanoflowers

The antioxidant activity of hNFs synthesized with *D. menziesii* extract was measured on the basis of the absorbance change due to oxidation DPPH [30]. For this study, increasing concentrations hNFs were added to DPPH (0.1 mM) at (between 0.165 and 10 mg/mL). The DPPH scavenging activity of hNFs were calculated by using the values measured at 517 nm after the incubation of the solution (30 min, dark medium).

$$\text{Scavenging activity } (\%) = \left[\left(\text{Abs}_{\text{control}} - \left(\text{Abs}_{\text{sample}} - \text{Abs}_{\text{blank}}\right)\right)\right] / \text{Abs}_{\text{control}} \times 100$$

$\text{Abs}_{\text{control}}$: distilled water, $\text{Abs}_{\text{blank}}$: ethanol (99.5%)

2.3 Catalytic Activities of Hybrid Nanoflowers

In order to evaluation the degradation of methylene blue and brilliant blue paints by hNFs via catalytic activity, 2 mg hNFs, dye and H_2O_2 were added to the each tubes containing PBS (pH 5, 7 and 9). The absorbances caused by hNFs in methylene blue and brilliant blue dyes were recorded at 664 nm and 590 nm, respectively. The dye degradation properties of hNFs depend on pH of PBS buffer and exposure time were calculated with the formula below [31].

$$\left[\text{Dye degradation } (\%) = \left[\left(\text{Abs}_1 - \text{Abs}_2\right) \times 100/\text{Abs}_1\right]\right.$$

Abs_1 first absorbance, Abs_2 last absorbance value.

3 Results and Discussion

3.1 Characterization of Hybrid Nanoflower

While hNFs were synthesized under the conditions when PBS pH was 7.4 and 9, but hNFs synthesis had not been realized under conditions where the pH was 5. FE-SEM images of hNFs synthesized by using *D. menziesii* (0.65 mL, 1 mL, and 1.65 mL) as organic component under the conditions in which the PBS pH was 7.4 is provided in Figs 1, 2, 3. It has been determined that the diameter of hNFs synthesized by the using of 0.65 mL of the *D. menziesii* extract was distributed in the range of 17–30 µm (Fig. 1). The diameter of hNFs synthesized by using 1 mL of the *D. menziesii* extract varied between 22 and 28 µm (Fig. 2). The diameter of hNFs synthesized at higher concentration (1.65 mL) was distributed in the range of 23–27 µm (Fig. 3). The average petal thickness of hNFs synthesized by using the same extract 0.65 mL, 1 mL and 1.65 mL were measured at 57 nm (Fig. 1), 38 nm (Fig. 2) and 48 nm (Fig. 3), respectively. Under the condition of PBS pH 9, diameters of hNFs synthesized with 65 mL, 1 mL and 1.65 mL algae extract were determined at 20–34 µm (Fig. 4), 31 µm (Fig. 5), and 9–34 µm (Fig. 6), respectively. Also, the average petal thicknesses of hNFs were also recorded at 45.6 nm (Fig. 4), 48 nm (Fig. 5), and 51 nm (Fig. 6) respectively.

Li et al. (2020) detailed the synthesis steps of hNFs in 4 steps [32]. During the nucleation phase (step 1), primary phosphate crystals are formed as a result of binding bivalent metals (Cu^{2+}, Ca^{2+}, Fe^{2+}, Mn^{2+}, etc.…) and phosphate (PO_4^{-3}). The interaction between positively charged bivalent metals and negatively charged phosphate is electrostatic binding. During the coordination and precipation phase (step 2 and step 3), nanopetals occur as a result of the coordination

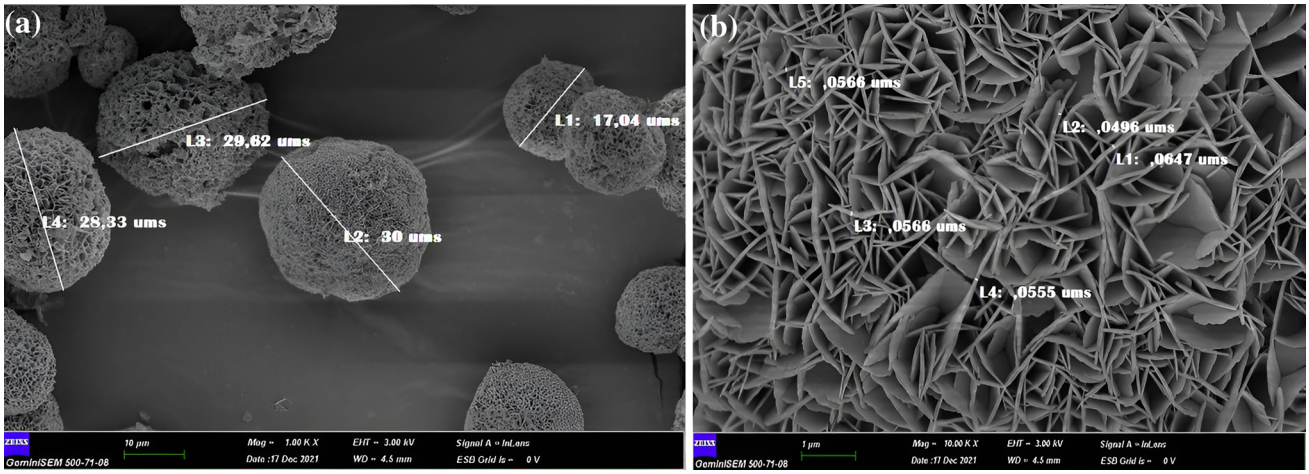

Fig. 1 FE-SEM images of hNFs synthesized by using 0.65 mL *D. menziesii* extract at PBS (pH:7.4)

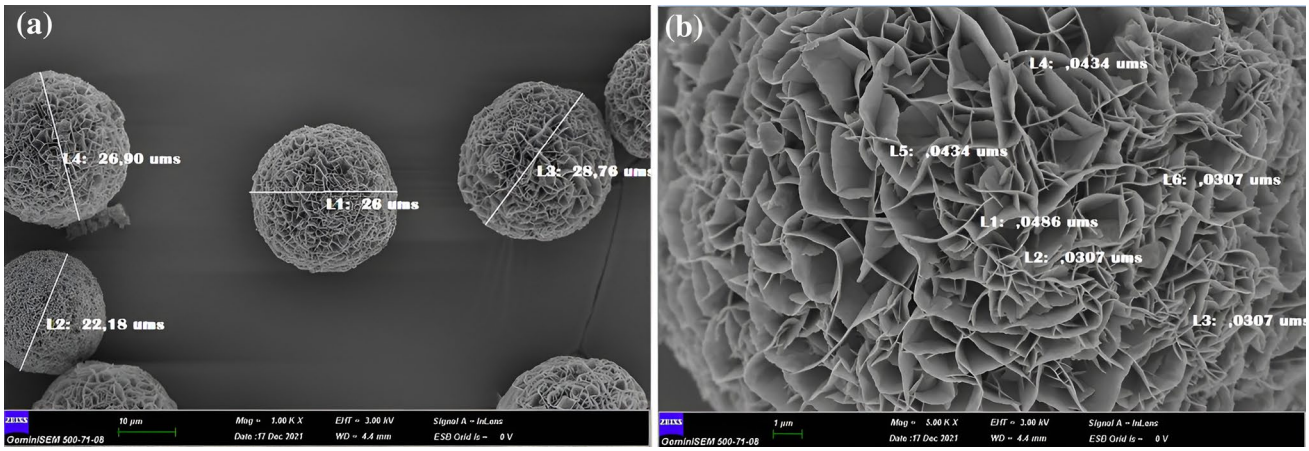

Fig. 2 FE-SEM images of hNFs synthesized by using 1 mL *D. menziesii* extract at PBS (pH:7.4)

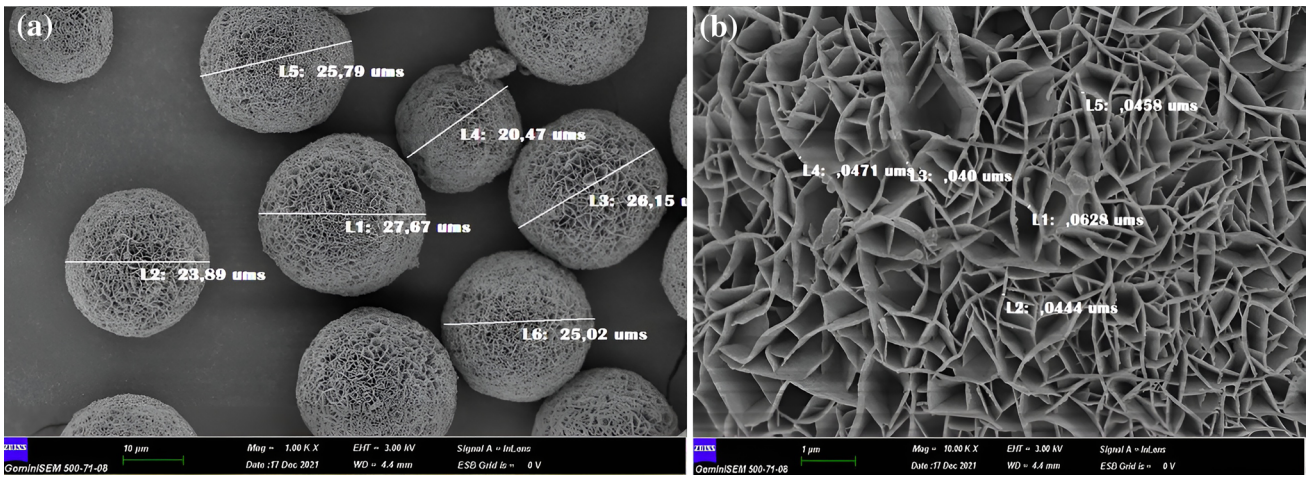

Fig. 3 FE-SEM images of hNFs synthesized by using 1.65 mL *D. menziesii* extract at PBS (pH:7.4)

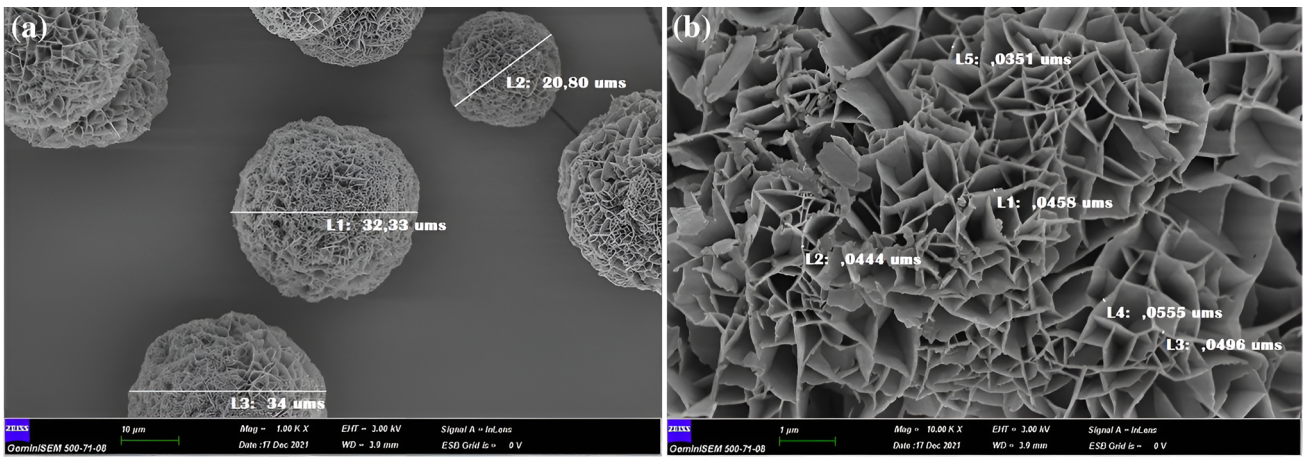

Fig. 4 FE-SEM images of hNFs synthesized by using 0.65 mL *D. menziesii* extract at PBS (pH:9)

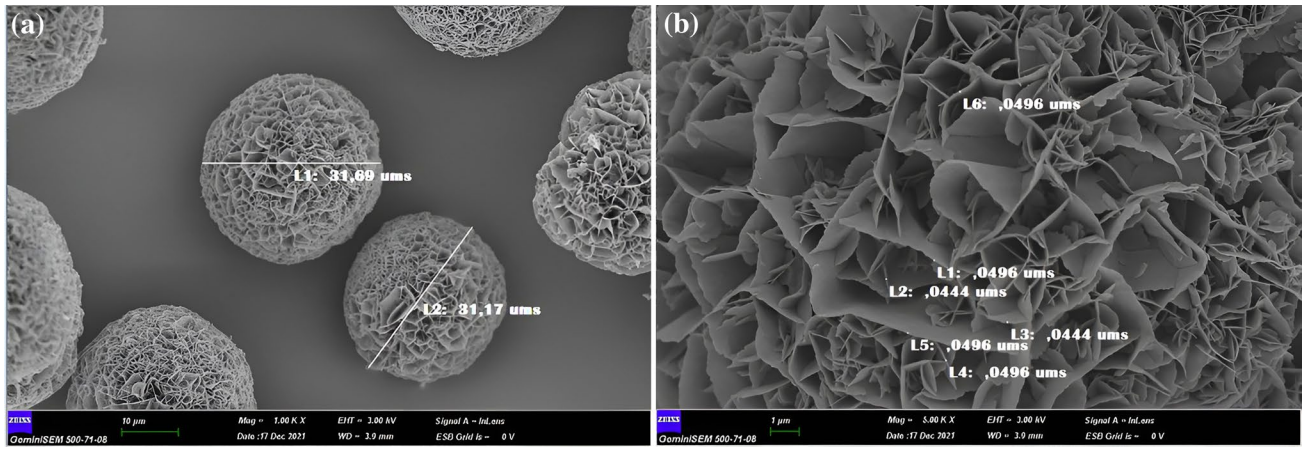

Fig. 5 FE-SEM images of hNFs synthesized by using 1 mL *D. menziesii* extract at PBS (pH:9)

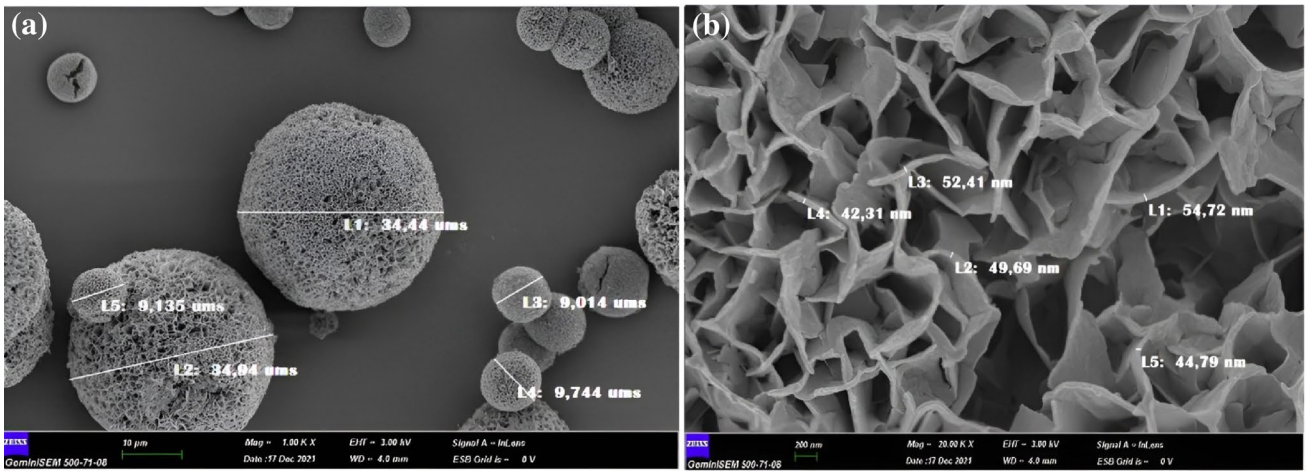

Fig. 6 FE-SEM images of hNFs synthesized by using 1.65 mL *D. menziesii* extract at PBS (pH:9)

of primary phosphate crystals and amide/N groups of organic compounds. In self assembly stage (Step 4) nanopetals aggregate together and as a result of anisotropic growth multi-layer hNFs occur. The kinetic and hierarchical synthesis of hNFs continues until the nanocrystals reach saturation [32, 33]. Parameters such as morphology and size of hNFs vary depending on many factors such as organic and inorganic components, reaction time, sonication, temprature of reaction, and medium pH [8]. Organic components used in synthesis are one of the main factors in the formation of hNFs, because the biomolecules function as glue in connection with metal phosphate crystals [32, 33]. Wu et al. synthesized hNFs using different amino acids as an organic component in the PBS buffer [34]. Researchers reported that (i) irregular composites are formed instead of hNF without amino acid in the medium, and (ii) different amino acids contain different side chains so amino acids affect the morphology of hNFs. The nucleation sites provided by organic components for the formation and nuclection of primary phosphate crystals in the synthesis phases of hNFs have a critical role [11]. Therefore, since the concentrations of organic components are associated with the nucleation sites, the organic component concentrations have key role on the synthesis of hNF and morphological structure. The effect of extract concentrations used for the synthesis of hNFs on the formation and morphology of hNFs has been revealed [22, 28, 35–37]. The pH of PBS buffer affects the charge of enzymes, proteins and other biomolecules used as an organic component in synthesis and this situation affects the coordination ability of biomolecules with metals and determines the synthesis and morphology of hNFs [32, 33]. Celik et al. reported that dopamine@Cu hNFs which is close to ideal flower morphology were synthesized under conditions when PBS pH value of 7.4 [38]. In addition, dopamine-based hNFs were not synthesized in extreme acidic (less than pH 5) and extreme basic PBS conditions (larger than

pH 10). In the other studies, the optimum pH values of the synthesis medium were determined for the synthesis of ideal hNFs [18, 28, 38]. According to our findings, uniform hNFs with ideal flower morphology were synthesized under the condition that PBS buffer pH was 7.4 and in the presence of 1.65 mL of extract. Our data are compatible with the literature and hNFs synthesized under optimum conditions were used in catalytic and antioxidant studies.

The Cu and other elemental components elements (C, O, and P) in the structure of hNFs synthesized by the use of the *D. menziesii* as an organic component are shown by EDX analysis (Fig. 7) and EDX mapping (Fig. 8), respectively. The % weight of the C, O, P and Cu elements contained in hNFs were determined at 56.94, 28.05, 4.22 and 10.78%, respectively. In addition, % atomic values of hNFs given as 69.72, 25.78, 2.01 and 2.50 respectively and are shown in Fig. 7, respectively.

Functional groups found in the structure of organic@inorganic hNFs were determined by vibrations observed in the FT-IR diagram (Fig. 9). The aromatic rings (C=C), aliphatic ether (C–O) presence in the structure of hNFs were determined by peaks observed at 1621 cm^{-1} and 1146 cm^{-1}, respectively. The presence of primary phosphate was revealed by vibrations observed at 1041 cm^{-1}, 987 cm^{-1}, 627 cm^{-1} and 558 cm^{-1} [21, 24, 28]. The XRD peaks (Fig. 10) that determined at 2θ = 9.21°, 13.16°, 18.7°, 20.42°, 24.15°, 30.76°, 34.11°, 37.28°, 41.52°, 45.96°, 54.08°, and 56.21° correspond to $Cu_3(PO_4)_2$ crystals (JCPDS Card 00–022 –0548) [39].

3.2 Antioxidant Activity of Hybrid Nanoflower

Antioxidants are important agents in order to combat with damage caused by oxidative stress. Unpaired electrons in the DPPH structure receive electron from the oxidants and become stable. Oxidants transfer electrons to DPPH and cause color change of DPPH and this changes are evaluated by reading spectrophotometer (at 517 nm) [40]. The antioxidant activity of hNFs *by D. menziesii* extract against DPPH was given in Fig. 11, and the IC_{50} value was determined at 950 µg/ mL ($R^2 = 0.855$).

Eskikaya et al. (2023), reported that iron NF and nanocubes have DPPH scavenging activity depending on concentration in accordance with our findings [41]. Altinkaynak et al., (2023) reported that *Aloe vera* extract and *A. vera* extract-based Cu hNFs have the similiar antioxidant activities [42]. Özdemir et al. reported that amino acid based bivalent metal (Co, Zn, and Cu) crystals absorbed DPPH at lower concentrations than amino acid @bivalent metal hNFs [43]. They also inform that cyteine@Zn hNFs have the highest antioxidant activity against DPPH among other different hNFs synhtesized coordination of amino acids (histidine, cyteine, asparagine, aspartic acid) and bivalent metals (Co, Zn and Cu). In that study, it was recorded that the synthesized hNFs inhibited free radicals and oxidative damage caused by their cause. Previous studies have shown that the concentration of nanomaterials, varieties of organic and inorganic components of hNFs significantly effect on DPPH scavenging activities.

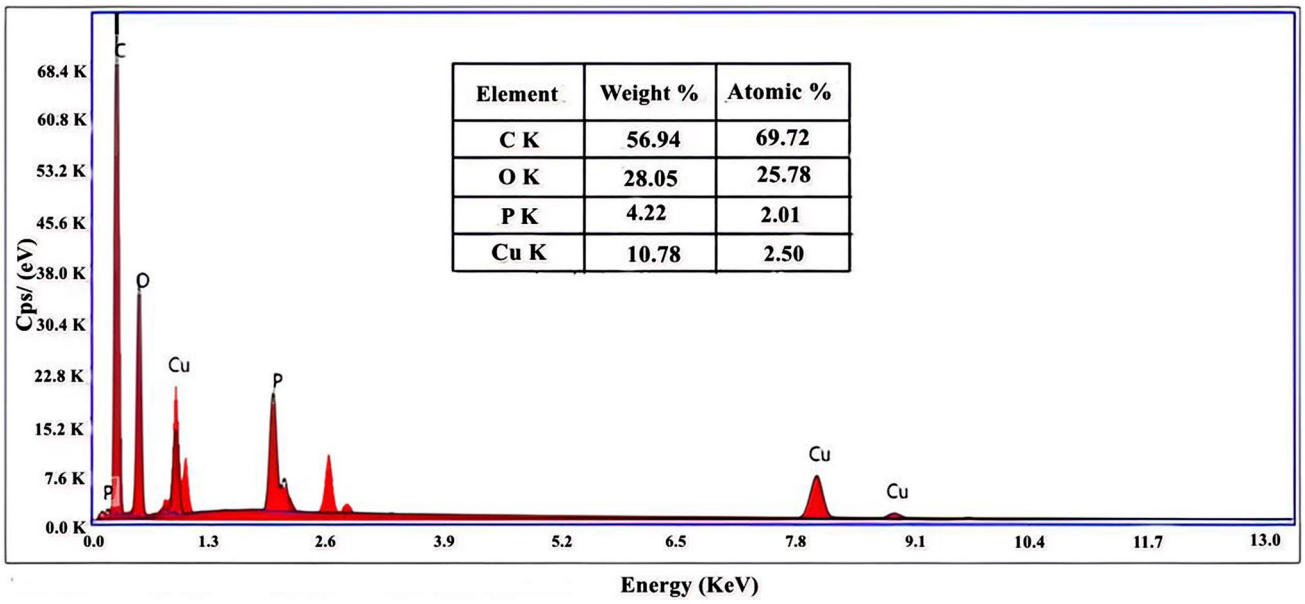

Fig. 7 EDX results of *D. menziesii* based hNFs

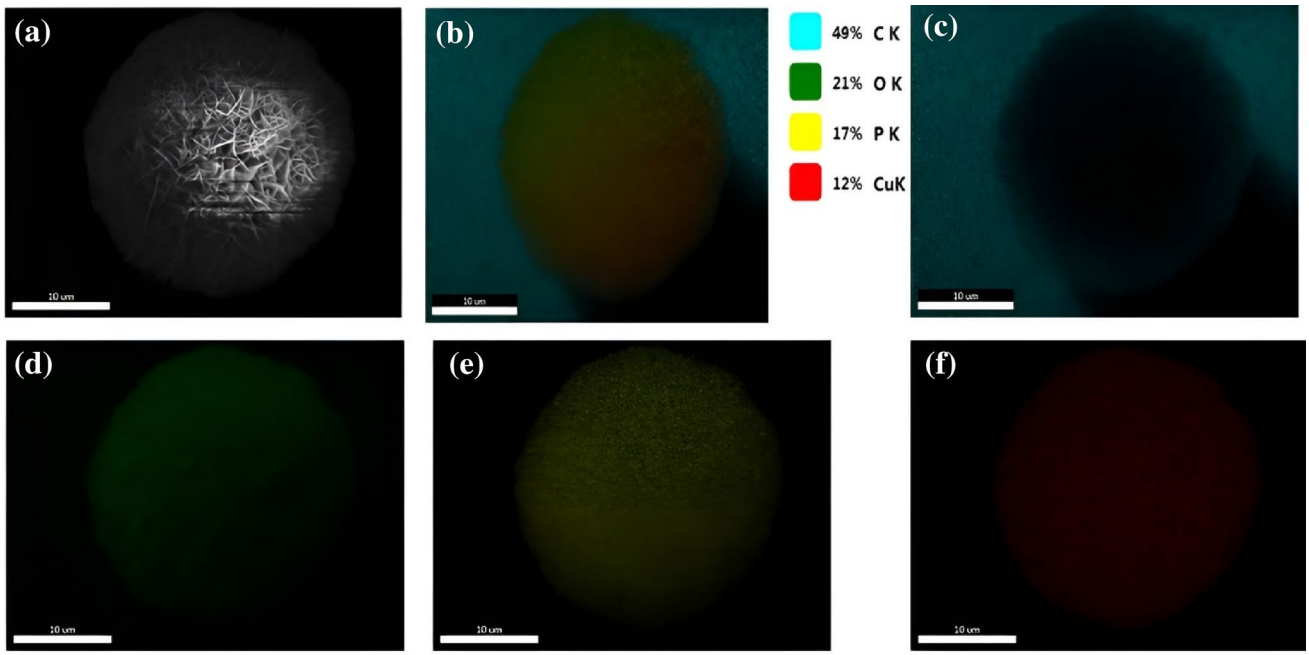

Fig. 8 EDX mapping of *D. menziesii* based hNFs. **a** image of hNFs, **b** elemental distrubution, **c** presence of C **d** presence of O **e** presence of P **f** presence of Cu (Color figure online)

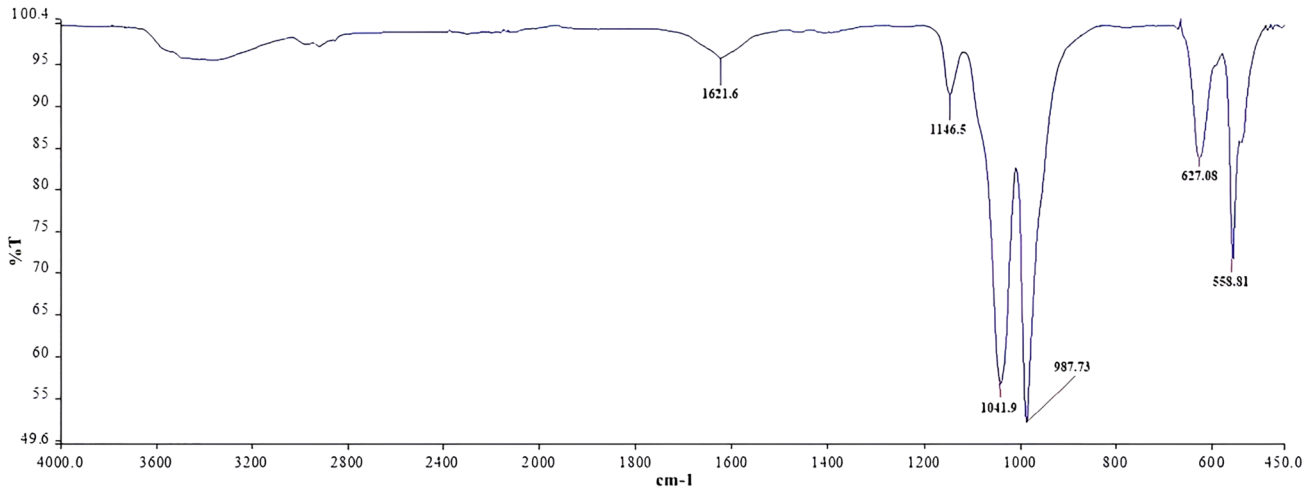

Fig. 9 FT-IR analysis of *D. menziesii* based hNFs

3.3 Catalytic Activity of Hybrid Nanoflower

D. menziesii-based hNFs caused catalytic degradation after 210 min of methylene blue 33.1%, 69.81%, and 58.58% at pH 5, 7 and 9 medium, respectively (Fig. 12a). Depending on the increasing time, absorbance changes of the dyes were recorded (Fig. 12b). Under the same pH conditions, 75.7%, 43.4% and 52.9% of brilliant blue was degraded, respectively (Fig. 13).

In previous studies, catalytic activities of Cu-based hNFs have been attributed to Fenton mechanism [27, 28, 34, 35, 44]. In Fenton mechanism, adsorption and degradation processes are inseparable mechanisms [41]. In this mechanism, the adsorption of the target pollutions at high concentration on the surface of hNF will increase the efficiency of degradation. hNFs have more reactive center for adsorption due to their hierarchical structures, which increases Fenton performance. Enhanced catalytic activity of urease@Cu hNFs were explained by the high surface areas of hNFs, their

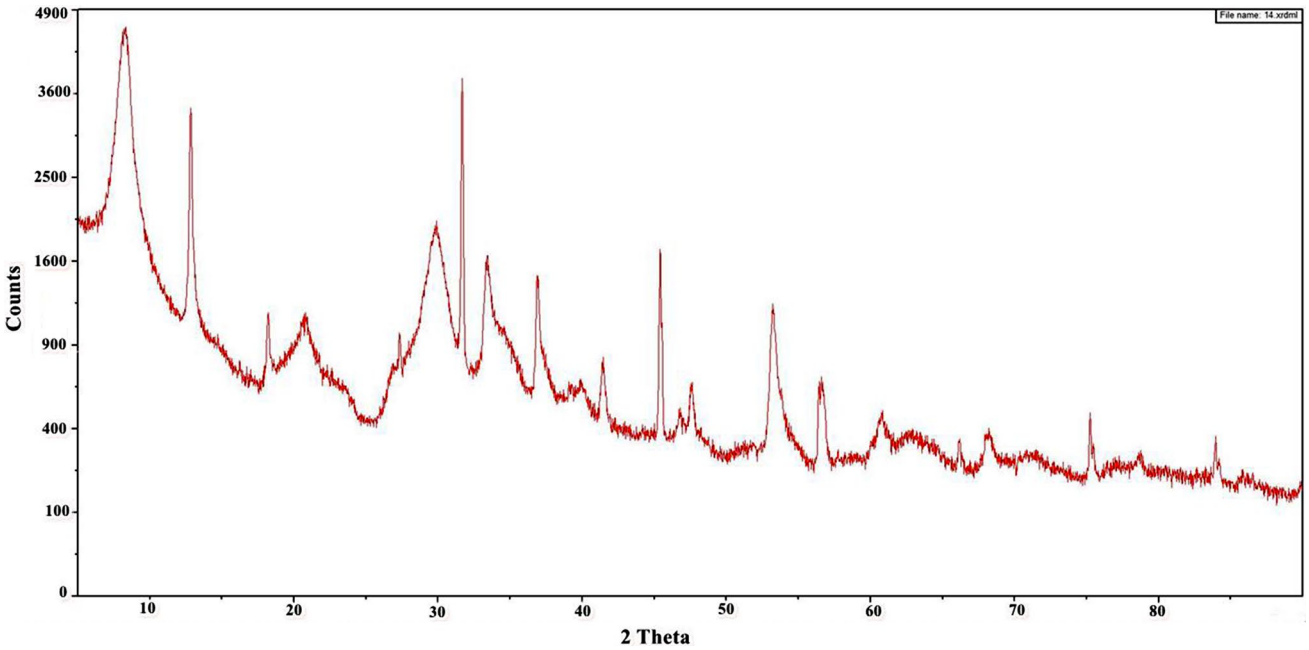

Fig. 10 XRD analysis of *D. menziesii* based hNFs

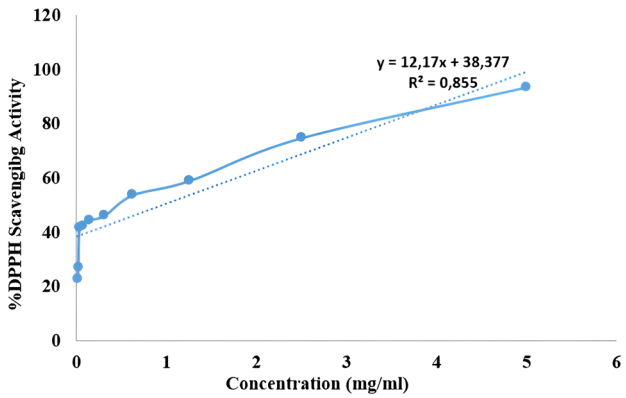

Fig. 11 Antioxidant activity of *D. menziesii* extract based hNFs

porous structures, the localization of the organic component in hNF and synergistic effects [12]. The malachite green degradation ability of *Euphorbia sanguinea* based Zn hNFs was explained via adsorption and photocatalytic mechanism [22]. [27] obtained *Usnea antarctica* ve *Usnea subfloridana* lichen extract by using distilled water and ethanol solvents [27]. It has been reported that Cu hNFs synthesized by using the extract of *U. subfloridana* (obtained with distilled water) the highest catalytic activity against guaiacol. Researchers suggested 45 that hNFs with a high surface area and porosity exhibit enhanced catalytic activity. They also reported that free radicals that occur as a result of the Fenton mechanism decompose the subsrate. Koca et al. reported that the Cu hNFs synthesized with *Ascoseria mirabilis* extract have catalytic activity through Fenton mechanism depending on exposure time [28]. Catalytic activities of catecholamines (epinephrine, dopamine, and norepinephrine)@Cu hNFs have been associated with the Fenton reaction, exposure time, and structural properties of hNFs [38]. Altınkaynak et al. reported that myoglobin@Zn (II) hNFs showed the highest peroxidase-like activity against ABTS under pH 4 medium [46]. They identified the highest catalytic activities of the hNFs against congo red, and evans blue dyes under the conditions of pH 6, and pH 4 respectively. Researchers have reported that the catalytic activities of the hNFs described by the Fenton mechanism were associated with the medium pH, temperature and hNF concentration. The Fenton mechanism is detailed in previous studies and given main catalytic process [27, 28, 35, 38, 46].

$$Cu^{2+} + H_2O_2Cu^{+} + HOO^{0} + H^{+} \quad \text{(a)}$$

$$Cu^{+} + H_2O_2Cu^{+2} + HO^{0} + OH^{+} \quad \text{(b)}$$

According to this mechanism, Cu^{+2} is reduced to Cu^{+1} after the reaction with H_2O_2 and free radicals formed as a result of Cu^{+1} and H_2O_2 reaction cause the oxidation of the substrate. For catalytic performance of nanomaterials, the medium pH has a key role. In an acidic medium, positively charged nanomaterials and cationic dye tends to repulsion [47]. For this reason, degradation activity of nanomaterials decreases [47]. The poor degradation of methylene blue dye in an acidic environment is due to this repulsive force. The high degradation of anionic brilliant blue dye in acidic

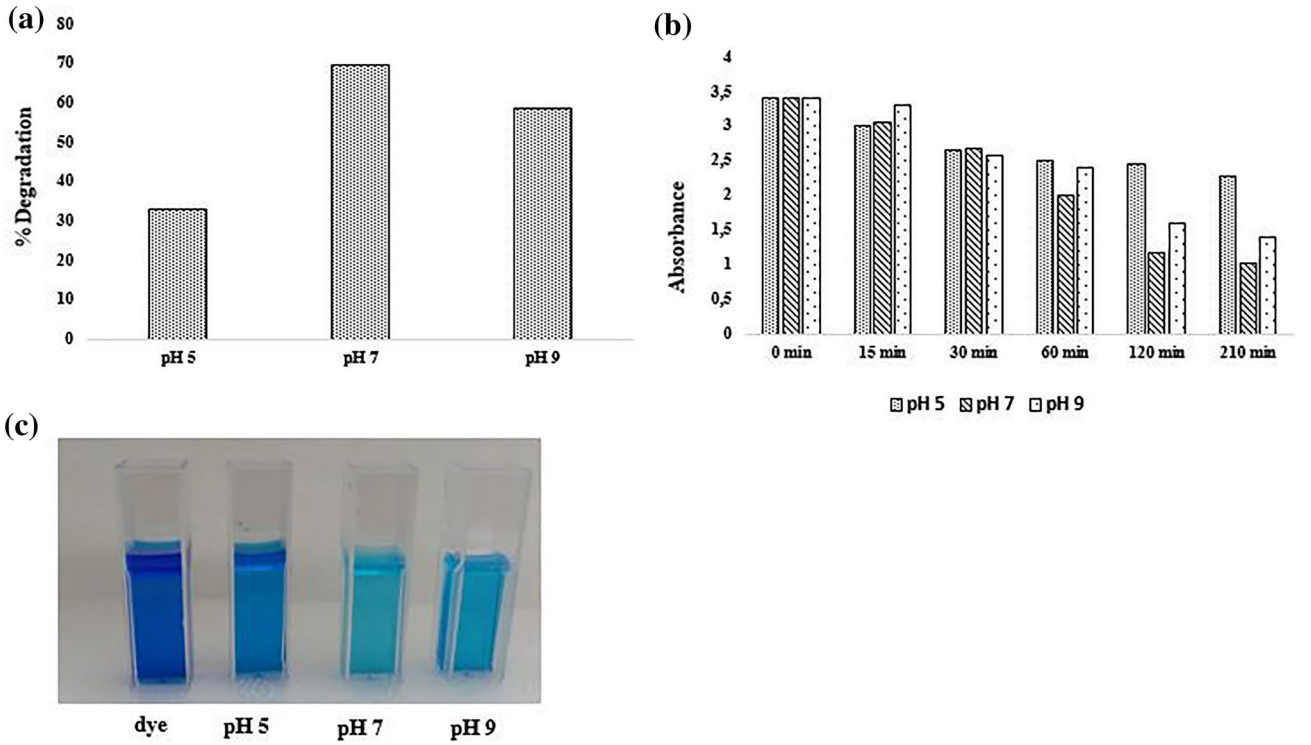

Fig. 12 Catalytic activity of *D. menziesii* extract based hNFs against to methylene blue (Color figure online)

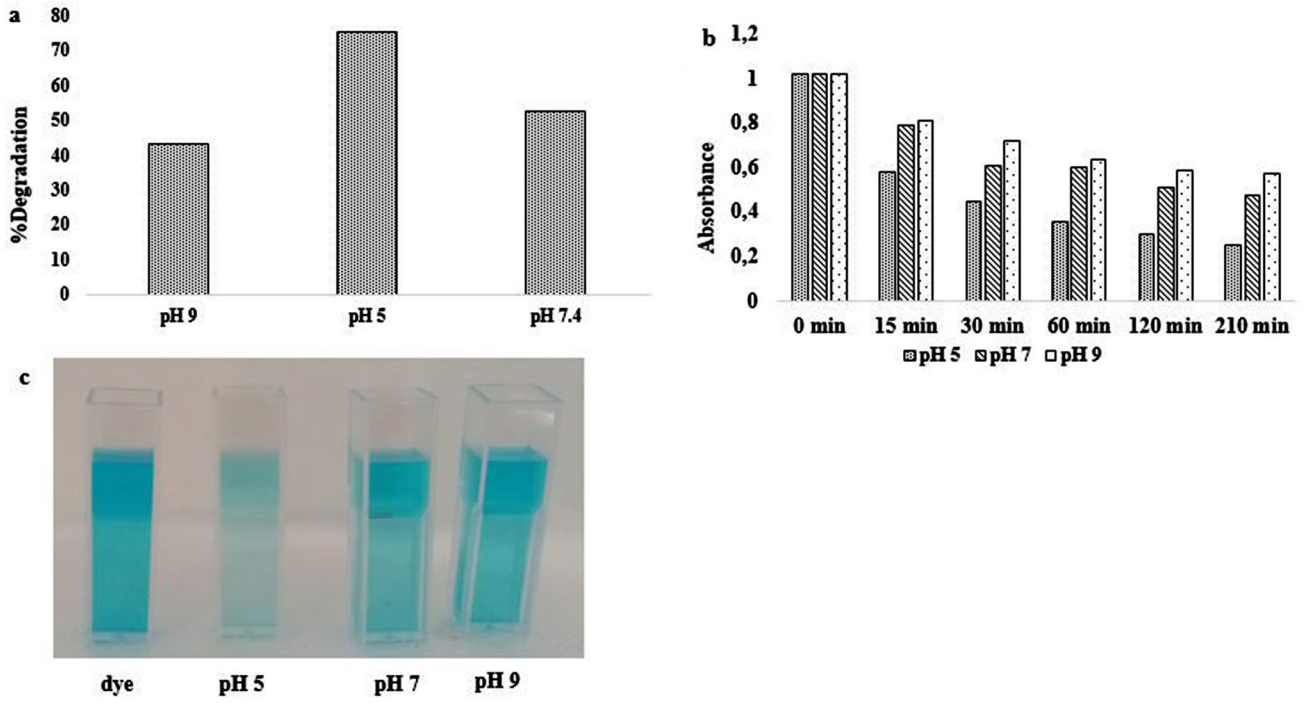

Fig. 13 Catalytic activity of *D. menziesii* extract based hNFs brilliant blue (Color figure online)

environment can also be explained by the interaction of the positively charged catalyst and the negatively charged dye.

4 Conclusion

hNFs were synthesized with coordination of *D. menziesii* extract and Cu + 2 depending on experimental parameters (extract concentration and medium pH). The ability to DPPH scevenging activity of (antioxidant property) has been demonstrated. We proved that hNFs exhibit catalytic activity depending on the medium pH and exposure time against methylene blue and brilliant blue dyes. The catalytic activity exhibited by hNFs in the presence of H_2O_2 was explained by the Fenton mechanism. The data of this study and similar studies might be useful for cheap, effective and one-step synthesis of hNFs by using various lichen, algae, fungal and plant extracts and applications of hNFs (biomedical, remediation, catalytic, etc.).

Acknowledgements The authors are thankful to the Dr. Musa Kar (Nevşehir Hacıbektas Veli University) for their valuable contribution to antioxidant studies.

Author Contributions Fatih Doğan KOCA: Planning of the study, Synthesis and characterization of Nanoflower, Writing.Haydar Matz MUHY: Antioxidant and catalytic activities of Nnaoflowers.Mehmet Gökhan HALICI: Planning of the study, Concept; methodology; writing; editing

Funding Not applicable

Data Availability Data is available on request from the authors.

Declarations

Conflict of Interest The authors have declared that no competing interests exist.

References

1. I. Hussain, N.B. Singh, A. Singh, S.C. Singh, Biotechnol. Lett. **38**, 545–560 (2016)
2. M. Sorbiun, E. Shayegan Mehr, A. Ramazani, J Mater Sci Mater Electron. **29**, 2806–2814 (2018)
3. S.R. Mishra, Md Ahmaruzzaman. Sep. Purif. Rev. (2022). https://doi.org/10.1080/15422119.2022.2096071
4. S.R. Mishra, V. Gadore, S. Ghotekar, M. Ahmaruzzaman, Int J Environ Anal Chem. (2023). https://doi.org/10.1080/03067319.2023.2186228
5. V. Gadore, S.R. Mishra, Md. Ahmaruzzaman, J. Hazard. Mater. **444**, 130301 (2023)
6. X. Li, J. Zhao, Z. Zhang, Y. Jiang, M. Bilal, Y. Jiang, S. Jia, J. Cui, Biochem. Eng. J. **158**, 107582 (2020)
7. J. Cui, Y. Zhao, R. Liu, C. Zhong, S. Jia, Sci. Rep. **6**, 27928 (2016)
8. J. Cui, S. Jia, Coord. Chem. Rev. **352**, 249–263 (2017)
9. H. Wen, L. Zhang, Y. Du, Z. Wang, Y. Jiang, H. Bian, J. Cui, S. Jia, J. CO_2 Util. **39**, 101171 (2020).
10. L. Zhong, X. Jiao, H. Hu, X. Shen, J. Zhao, Y. Feng, C. Li, Y. Du, J. Cui, S. Jia, Renew. Energ. **171**, 825–832 (2021)
11. J. Ge, J. Lei, R.N. Zare, Nature Nanotech. **7**, 428–432 (2012)
12. B. Somturk, I. Yilmaz, C. Altinkaynak, A. Karatepe, N. Özdemir, I. Ocsoy, Enzym Microb Technol. **86**, 134–142 (2016)
13. B. Sun, Z. Wang, X. Wang, M. Qiu, Z. Zhang, Z. Wang, J. Cui, S. Jia, Int. J. Biol. Macromol. **166**, 601–610 (2021)
14. Z. Zhang, Y. Du, G. Kuang, X. Shen, X. Jia, Z. Wang, Y. Feng, S. Jia, F. Liu, M. Bilal, J. Cui, Renew. Energ. **197**, 110–124 (2022)
15. Z. Wang, R. Wang, Z. Geng, X. Luo, J. Jia, S. Pang, X. Fan, M. Bilal, J. Cui, Crit. Rev. Biotechnol. (2023). https://doi.org/10.1080/07388551.2023.2189548
16. Y. Liu, Z. Wang, Y. Feng, Y. Jiao, L. Zhong, G. Kuang, Y. Du, M. Bilal, S. Jia, J. Cui, Sustain. Mater. Technol. **32**, e00432 (2022)
17. P. Li, J. Jia, Z. Geng, S. Pang, R. Wang, M. Bilal, H. Bian, J. Cui, S. Jia, Particuology. **83**, 63–70 (2023)
18. N.I. Alhayali, N.K. Ozpozan, S. Dayan, N. Ozdemir, B.S. Yilmaz, Polyhedron **194**, 114888 (2021)
19. T.D. Tran, P.T. Nguyen, T. Nguyen Le, M.I. Kim, Biosens Bioelectron. **182**, 113187 (2021).
20. R. Cai, S. Zhang, L. Chen, M. Li, Y. Zhang, N. Zhou, ACS Appl. Mater. Interfaces **13**, 4905–4914 (2021)
21. A. Demirbas, Indian. J. Microbiol. **61**, 324–330 (2021)
22. A.C. Ekennia, D.N. Uduagwu, N.N. Nwaji, O.O. Oje, C.O. Emma-Uba, S.I. Mgbii, O.J. Olowo, O.L. Nwanji, J. Inorg. Organomet. Polym. **31**, 886–897 (2021)
23. A.H. Al Sharie, T. El-Elimat, R.S. Darweesh, S. Swedan, Z. Shubair, R. Al-Qiam, H. Albarqi, Appl Organomet Chem **34**, e5667 (2020).
24. B. Karslı, I.S. Uras, B. Konuklugil, A. Demirbas, IEEE Trans. Nanobioscience **22**, 523–528 (2023)
25. N. Shahabadi, S. Zendehcheshm, F. Khademi, K. Rashidi, K. Chehri, M. Fatahi Dehpahni, J Environ Chem Eng. **9**, 105215 (2021).
26. I.S. Uras, B. Karsli, B. Konuklugil, I. Ocsoy, A. Demirbas, Sustainability. **15**, 4638 (2023)
27. A. Demırbas, B. Karslı, S. Dadi, F.D. Koca, M.G. Halıcı, I. Ocsoy, ChemistrySelect **7**, e202202715 (2022)
28. F.D. Koca, H.M. Muhy, M.G. Halici, B. Gozcelıoglu, B. Konuklugil, Appl. Nanosci. **13**, 4787–4794 (2023)
29. N. González-Ballesteros, J.B. González-Rodríguez, M.C. Rodríguez-Argüelles, M. Lastra, Polar Sci. **15**, 49–54 (2018)
30. O.C. Güven, M. Kar, F.D. Koca, J. Inorg. Organomet. Polym. Mater. **32**, 1026–1032 (2022)
31. C. Altinkaynak, S. Tavlasoglu, R. Kalin, N. Sadeghian, H. Ozdemir, I. Ocsoy, N. Özdemir, Chemosphere **182**, 122–128 (2017)
32. Y. Li, H. Wu, Z. Su, Coord. Chem. Rev. **416**, 213342 (2020)
33. J. Chen, Z. Guo, Y. Xin, Z. Gu, L. Zhang, X. Guo, Coord. Chem. Rev. **489**, 215191 (2023)
34. Z.F. Wu, Z. Wang, Y. Zhang, Y.L. Ma, C.Y. He, H. Li, L. Chen, Q.S. Huo, L. Wang, Z.Q. Li, Sci. Rep. **6**, 22412 (2016)
35. N. Ildiz, A. Baldemir, C. Altinkaynak, N. Özdemir, V. Yilmaz, I. Ocsoy, Enzyme Microb. Technol. **102**, 60–66 (2017)
36. C. Altinkaynak, N. Ildız, A. Baldemir, N. Özdemir, V. Yılmaz, I. Ocsoy, Derim. **36**, 159–167 (2019)
37. U. Koca Caliskan, C. Dönmez, N. Eruygur, F. Ayaz, C. Altinkaynak, N. Özdemir, Chem Biodivers. **19**, e202200476, (2022).
38. C. Celik, N. Ildiz, I. Ocsoy, Sci. Rep. **10**, 2903 (2020)
39. S.S. Maurya, S.S. Nadar, V.K. Rathod, Environ. Technol. Innov. **19**, 100798 (2020)
40. A.A. Sumra, M. Zain, T. Saleem, G. Yasin, M.F. Azhar, Q.U. Zaman, V. Budhram-Mahadeo, H.M. Ali, Plants. **12**, 1578 (2023)
41. O. Eskikaya, S. Özdemir, S. Gonca, N. Dizge, D. Balakrishnan, F. Shaik, N. Senthilkumar, Appl. Nanosci. **13**, 5421–5433 (2023)

42. C. Altınkaynak, E. Haciosmanoglu, M. Ekremoglu, M. Hacioglu, N. Özdemir, J. Biosci. Bioeng. **135**, 321–330 (2023)
43. N. Özdemir, C. Altınkaynak, M. Türk, F. Geçili, S. Tavlaşoğlu, Polym. Bull. **79**, 9697–9716 (2022)
44. A. Demirbas, B. Karslı, I. Ocsoy, Chem Biodivers. e202300743 (2023). https://doi.org/10.1002/cbdv.202300743
45. Y. Mei, Y. Zhang, J. Li, X. Deng, Y. Yang, Q. Yang, B. Jiang, B. Xin, T. Yao, J. Wu, J. Alloys Compd. **904**, 163879 (2022)
46. C. Altınkaynak, M. Türk, N. Yangin, N. Özdemir, Chem. Biodivers. **20**, e202201136 (2023)
47. S. Begum, S.R. Mishra, Md. Ahmaruzzaman, Inorg. Chem. Commun. **143**, 109721 (2022)